2010 IEEE International Conference on Robotics and Automation
Anchorage Convention District
May 3-8, 2010, Anchorage, Alaska, USA

Improving the Kinematic Performance of the SCARA-Tau PKM

Mats Isaksson, Torgny Brogårdh, Ivan Lundberg, and Saeid Nahavandi

Abstract— **One well acknowledged drawback of traditional parallel kinematic machines (PKMs) is that the ratio of accessible workspace to robot footprint is small for these structures. This is most likely a contributing reason why relatively few PKMs are used in industry today. The SCARA-Tau structure is a parallel robot concept designed with the explicit goal of overcoming this limitation and developing a PKM with a workspace similar to that of a serial type robot of the same size. This paper shows for the first time how a proposed variant of the SCARA-Tau PKM can improve the usability of this robot concept further by significantly reducing the dependence between tool platform position and orientation of the original concept. The inverse kinematics of the proposed variant is derived and a comparison is made between this structure and the original SCARA-Tau concept, both with respect to platform orientation changes and workspace.**

I. INTRODUCTION

The interest in parallel kinematic machines (PKMs) and the number of innovative prototypes created by the research community is steadily increasing. A useful source of many proposed PKMs is [1] where drawings of 178 suggested structures can be found. Even so, it remains a fact that comparatively few of the proposed PKMs have resulted in an industrial product. Possible reasons for this have been discussed in [2], [3].

One of the few PKMs that has made it to a successful product for a larger industrial use is the DELTA structure invented by Clavel [4]. Robots of this type are manufactured by, for example, ABB, Bosch, Manz and Festo. The motors of the DELTA structure are placed on the non-moving base and only tensile or compressive forces are present in the lower arm links. This allows for a very lightweight robot with much higher speed and acceleration in relation to installed actuator power compared to competing serial type robots. DELTA robots are mainly used for high speed pick-and-place and assembly applications in predominantly the food, pharmaceutical, and electronics industries.

Although successful, the DELTA structure does have a relatively small usable workspace. Many industrial applications would benefit from a PKM with larger workspace. However, trying to build on the success of the DELTA robot by scaling up the structure will be difficult. The reason is that most DELTA structures used in industry are optimized to obtain a wide and shallow workspace, which is achieved by a large ratio between the lengths of the passive and actuated arms. This means that a proportional increase of the arm lengths leads to a corresponding increase of the distance between the usable workspace and the robot actuators. Because of this a taller, bulkier platform is needed which has many disadvantages, the most obvious being increased cost, reduced stiffness, lower eigenfrequencies, and increased weight.

Reference [5] describes a systematic approach to finding new parallel structures that build on the positive qualities of the DELTA structure, while overcoming some of its limitations. One of the proposed structures resulting from this approach is the SCARA-Tau structure, patented by ABB Robotics [6]. The kinematics of the SCARA-Tau robot has been published before [7], where a straightforward model is used to derive the nominal kinematics and a Denavit-Hartenberg model with 72 parameters used for error analysis.

This paper focuses on a proposed variant of the SCARA-Tau robot, presented in [8]. A new approach to derive the kinematics of the SCARA-Tau structure is presented, making it possible to describe the kinematics of the original SCARA Tau just by setting one parameter of the proposed SCARA-Tau variant to zero. Moreover, the inverse kinematics that include all kinematic error parameters of the SCARA Tau variant has been derived. The inverse nominal kinematic models are used in simulations in order to make a quantitative evaluation of the benefits of the SCARA-Tau variant proposed in [8].

II. THE SCARA-TAU CONCEPT

A. The Tau concept

The Tau family of PKMs are based on a number of patents [6], [9], [10]. The basis of the Tau concept is a grouping of the passive lower arm links in groups of 3, 2 and 1 links respectively, where each group nominally has parallel links of equal length and is actuated independently. The advantage of this 3/2/1 grouping compared to the 2/2/2 grouping of the DELTA concept is that the restrictions on where to place and how to orient the joints can be significantly relaxed, thereby allowing a lot more flexibility and opening up possibilities for new PKM structures.

Different prototypes based on a gantry version of the Tau concept using prismatic actuators have been built and studied extensively by separate groups of researchers [11], [12].

B. The original SCARA-Tau robot

A prototype based on the SCARA-Tau concept, shown in Fig. 1, was built by ABB Robotics in 2000. The robot is presently being studied at Deakin University, Australia, in a joint research project between Deakin University, ABB Robotics and Boeing Australia.

M. Isaksson and S. Nahavandi are with the Center for Intelligent Systems Research (CISR), Deakin University, Australia. E-mail: mei@deakin.edu.au, saeid.nahavandi@deakin.edu.au. T. Brogårdh and I. Lundberg are with ABB Corporate Research, Sweden. E-mail: torgny.brogardh@se.abb.com, ivan.lundberg@se.abb.com.

Fig. 1. The SCARA-Tau robot prototype. The height of the robot is 2.25 meters.

The SCARA-Tau robot is built on the fact that unlike the 2/2/2 structure of the DELTA robot, the 3/2/1 structure allows a common axis of rotation for the three actuated upper arms with constant platform pitch and roll angles. Therefore the 3/2/1 lower arm link configuration opens up for a parallel robot with similar workspace as a traditional serial type SCARA robot.

The prototype in Fig. 1 utilizes three different types of joints. There are three actuated 1-DOF rotational joints between the central column and the upper arms. The joints connecting the lower arm links and the moving platform are 2-DOF universal joints (could also be 3-DOF), while somewhat heavier 3-DOF universal joints connect the upper and lower arms. Presently the robot has 3 DOFs and can move independently in the 3 translational directions. The platform is connected by a double parallelogram to the lowest upper arm and by a vertical parallelogram to the middle upper arm. This arrangement means that the pitch and roll angles of the moving platform are constant while the platform yaw angle is dependent on the position of the lowest upper arm.

The SCARA-Tau robot has all the typical advantages of a high performance PKM. Since the actuators are placed on the non-moving base and the six lower arm links will only transmit tensile and compression forces and can be made of light weight carbon fibre rods, the mass moved by the motors is low. Joint errors are non-accumulative leading to higher accuracy. It is possible to use identical drive lines and identical upper and lower arms so the number of different parts needed to produce the robot can be kept low, reducing the production cost. The structural stiffness and mechanical bandwidth of the robot is high compared to a serial robot of the same size. In addition to these typical PKM advantages the SCARA-Tau robot has some additional positive qualities. The major advantage is that the working range is comparative to a serial type robot of similar size and that the workspace contains no parallel singularities. The SCARA-Tau robot also has the possibility for infinite rotation around the base. Other advantages of the robot are related to the floor mounted design which allows easy cabling solutions, easy service and makes it uncomplicated to move the robot when changing a manufacturing line. The fact that the robot footprint and workspace are similar to those of a serial type robot of the same size also means that the SCARA-Tau fits easily into automation systems where traditional SCARA robots are used today.

C. Triangular link SCARA-Tau

The nominal platform orientation of the original SCARA-Tau robot has constant pitch and constant roll, while the yaw angle is dependent on the position of the lowest upper arm.

In applications where the robot performs its tasks in the vertical direction towards a horizontal plane, varying tool yaw orientation is either no problem, as in laser cutting, or it can be compensated for by means of an additional 4th axis, as for traditional SCARA robots. The latter is typically done in applications like pick-and-place and palletizing.

However, in applications where the robot instead works in directions parallel to the horizontal plane, like for example measurements or machine tending, the workspace will be limited by this platform reorientation. A wrist with a large working range would help, but in positions like the one shown in Fig. 2(a), even a wrist with very large working range would have difficulties to rotate a tool to, for example, the negative y-direction.

The limitations of the original SCARA-Tau concept due to intrinsic platform reorientation are mentioned in [8] and a modification, replacing the horizontal part of the double parallelogram with a triangular link arrangement according to Fig. 3, is proposed. The vertical distances of u_1 - u_3 and u_2 - u_3 are equal to the vertical distances of p_1 - p_3 and p_2 - p_3 respectively, which means the vertical parallelogram remains and that the platform pitch angle remains constant over the workspace just as for the original SCARA-Tau concept. The difference between this arrangement and the original SCARA-Tau structure is that the platform yaw angle in this case is not fixed in relation to the angle of the lowest upper arm U_1 but can rotate around the axis R defined by the centers of the 3 joint positions u_1, u_2 and u_3.

The main benefit of the link arrangement in Fig. 3 is that the intrinsic yaw rotation of the platform over the workspace is reduced compared to the original SCARA-Tau structure. Fig. 2(b) shows the triangular link SCARA-Tau plotted in the same position as the original SCARA-Tau prototype in Fig. 2(a). Comparing these two plots demonstrates how the two structures give different platform orientation in the same position. As can be seen, at least in this position close to the outer limits of the workspace, the triangular link arrangement gives a more useful platform orientation. A comparison of the platform orientation over the whole workspace between the two variants is shown later in this paper.

Another benefit of the triangular link arrangement that can be seen if comparing Fig. 2(a) and Fig. 2(b) is that the horizontal parallelogram of the original SCARA-Tau structure approaches its working range boundaries in the regions close to the outer workspace limits of the robot, while this is not an issue for the triangular link variant. This advantage is also true in the regions close to the inner workspace limits of the robot.

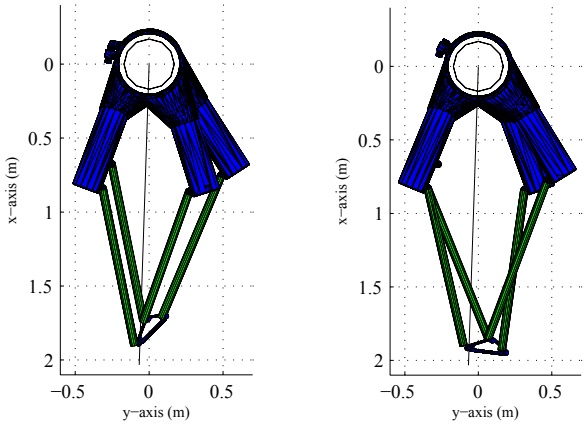

(a) SCARA-Tau prototype (b) Triangular link SCARA-Tau

Fig. 2. A top view of the SCARA-Tau prototype (a) and the proposed triangular link SCARA-Tau robot (b) in the same position. In both plots a radial line through the center of the base column and the center of the tool coordinate system has been plotted. An optimal platform orientation would in all positions form a 90 degree angle with such a line.

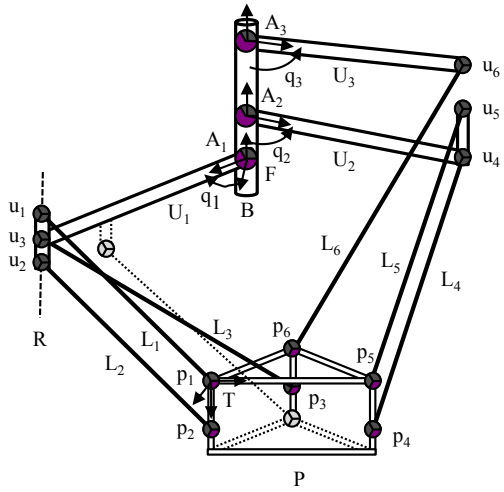

Fig. 3. The bodies and joint positions of the proposed triangular link SCARA-Tau variant. Compared to the SCARA-Tau prototype only the joint positions u_3 and p_3 are moved. The corresponding positions for the SCARA-Tau prototype are indicated in the figure. Also included in the figure are the three coordinate systems A_1, A_2, A_3, the tool coordinate system T, and the fixed coordinate system F.

III. KINEMATIC MODELING

A. Introduction

The proposed triangular SCARA-Tau robot can be separated into 11 rigid bodies connected by joints. The bodies, shown in Fig. 3, are:

- 1 Base column (B)
- 3 Upper arms (U_1, U_2, U_3)
- 6 Lower arm links (L_1, L_2, L_3, L_4, L_5, L_6)
- 1 Moving platform (P)

The only modifications compared to the original SCARA-Tau concept is a change of the two joint positions u_3 and p_3. The positions of these two joints for the SCARA-Tau prototype are indicated in Fig. 3.

B. Joint positions on the upper arms

In order to simplify the kinematic modeling, a coordinate system A_i is attached to each actuated upper arm U_i as shown in Fig. 3. The z-axis of each of these coordinate systems is set to be the axis of rotation for the corresponding upper arm, with positive direction being upwards. The x-axis is decided to be perpendicular to the z-axis in the direction of one of the joint positions on the arm and the y-axis is then decided according to the right hand rule. Using these coordinate systems the six joint positions on the upper arms in Fig. 3 can be described using 12 parameters according to

$$\begin{aligned} {}^{A_1}u_1 &= [u_{1x}, u_{1y}, u_{1z}]^T \\ {}^{A_1}u_2 &= [u_{2x}, u_{2y}, u_{2z}]^T \\ {}^{A_1}u_3 &= [u_{3x}, 0, 0]^T \\ {}^{A_2}u_4 &= [u_{4x}, 0, 0]^T \\ {}^{A_2}u_5 &= [u_{5x}, u_{5y}, u_{5z}]^T \\ {}^{A_3}u_6 &= [u_{6x}, 0, 0]^T \end{aligned} \tag{1}$$

The joint position u_3 for the SCARA-Tau prototype is also marked in Fig. 3. The description (1) defining the joint positions on the upper arms is valid also for the prototype, even if the vertical position of the coordinate system A_1 has to be moved so its x-axis remains in the direction of u_3.

C. Fixed coordinate system

A fixed coordinate system F is introduced and chosen to be identical to the arm coordinate system A_1, except for a rotation q_1. To describe the orientation of the arm coordinate systems A_2 and A_3 in relation to the fixed coordinate system, F, an Euler XYZ angles representation, with successive rotations $A_{i\phi}$, $A_{i\theta}$ and $A_{i\psi}$ about the x-, y- and z-axis, is used. For the SCARA-Tau robot $A_{i\phi}$ and $A_{i\theta}$ will be constant and equal to $A_{i\phi 0}$ and $A_{i\theta 0}$ respectively, while $A_{i\psi}$ is given by the sum of a constant value $A_{i\psi 0}$ and the joint position for the corresponding upper arm q_i, which is measured from the positive x-axis of the fixed coordinate system. The positions of the upper arm joints in the fixed frame can be represented as

$$\begin{aligned} {}^F u_1 &= {}^F R_{A_1}{}^{A_1} u_1 \\ {}^F u_2 &= {}^F R_{A_1}{}^{A_1} u_2 \\ {}^F u_3 &= {}^F R_{A_1}{}^{A_1} u_3 \\ {}^F u_4 &= {}^F O_{A_2} + {}^F R_{A_2}{}^{A_2} u_4 \\ {}^F u_5 &= {}^F O_{A_2} + {}^F R_{A_2}{}^{A_2} u_5 \\ {}^F u_6 &= {}^F O_{A_3} + {}^F R_{A_3}{}^{A_3} u_6 \end{aligned} \tag{2}$$

where

$$
\begin{aligned}
{}^{F}O_{A_2} &= [A_{2x}, A_{2y}, A_{2z}]^T \\
{}^{F}O_{A_3} &= [A_{3x}, A_{3y}, A_{3z}]^T \\
{}^{F}R_{A_1} &= R_z(q_1)^T \\
{}^{F}R_{A_2} &= (R_z(q_2 + A_{2\psi 0}) R_y(A_{2\theta 0}) R_x(A_{2\phi 0}))^T \\
{}^{F}R_{A_3} &= (R_z(q_3 + A_{3\psi 0}) R_y(A_{3\theta 0}) R_x(A_{3\phi 0}))^T
\end{aligned} \tag{3}
$$

The coordinate systems F and A_i are drawn in Fig. 3. The equations (2) and (3) are valid also for the SCARA-Tau prototype even if A_{2z} and A_{3z} are not the same since the positions of the coordinate systems A_1 and F are different. For both the proposed triangular link SCARA-Tau and the SCARA-Tau prototype the nominal values of A_{2x}, A_{2y}, A_{3x}, A_{3y}, $A_{2\phi 0}$, $A_{2\theta 0}$, $A_{2\psi 0}$, $A_{3\phi 0}$, $A_{3\theta 0}$ and $A_{3\psi 0}$ are all zero.

D. Joint positions on the moving platform

Each joint position on the upper arms, u_i, is connected via a lower arm link, L_i, to a corresponding joint position on the moving platform, p_i, as shown in Fig. 3.

A tool coordinate system T with origin in the joint position p_1 is introduced. The x-axis of the tool coordinate system is defined by the p_1 to p_2 direction and the z-axis normal to the plane created by p_1, p_2 and p_5, pointing away from the robot, while the y-axis is defined according to the right hand rule. The joint positions in the tool coordinate system can be represented by the 12 parameters below

$$
\begin{aligned}
{}^{T}p_1 &= [0,0,0]^T \\
{}^{T}p_2 &= [p_{2x}, 0, 0]^T \\
{}^{T}p_3 &= [p_{3x}, p_{3y}, p_{3z}]^T \\
{}^{T}p_4 &= [p_{4x}, p_{4y}, p_{4z}]^T \\
{}^{T}p_5 &= [p_{5x}, p_{5y}, 0]^T \\
{}^{T}p_6 &= [p_{6x}, p_{6y}, p_{6z}]^T
\end{aligned} \tag{4}
$$

The position of the tool coordinate system in the fixed coordinate system is given by three translations x, y, z. For the tool coordinate system orientation Euler ZYZ convention is used and the orientation in relation to the fixed coordinate system is decided by three successive rotations, ϕ, θ and ψ. Using these definitions the joint positions in the fixed coordinate system are given by

$$
\begin{aligned}
{}^{F}p_i &= {}^{F}O_T + {}^{F}R_T \, {}^{T}p_i \\
{}^{F}O_T &= [x, y, z]^T \\
{}^{F}R_T &= (R_z(\psi) R_y(\theta) R_z(\phi))^T
\end{aligned} \tag{5}
$$

The equations (4) and (5) are valid also for the SCARA-Tau prototype and the values in (4) except p_{3x} are all the same.

E. Lower arms

The remaining bodies to be given parameterized descriptions are the lower arm link chains. How to model these link chains depends on the accuracy of the used joints. The proposed triangular link SCARA-Tau variant would be built utilizing universal joints with two and three DOFs similar to the SCARA-Tau prototype. The universal joints used for the prototype are of the INA brand from the Schaeffler Group[13]. The reason for using universal joints instead of ball joints is that they usually have larger working range. The use of universal joints introduces the problem of universal joint offsets. Instead of modeling each lower arm with only the arm length, each arm can be modeled as a link chain with 5 rotary joints using 5×3 parameters per lower arm. For the SCARA-Tau prototype, the nominal offset of the used joints is only 3 micrometers when the joints are not carrying any load. When a joint is loaded the flexibility of the bearings also contributes to the joint offset. The total stiffness of the prototype joints is 50 N/micrometer. Joints with an offset of less than 1 micrometer and stiffness of more than 100 N/micrometer have been developed in the EU-project SMErobot™ [14]. If the requirements on accuracy are very high and a contact application, creating high loads on the joints, is studied, offset errors and compliance of the joints could be modeled and compensated for.

In order to study the difference between the SCARA Tau variants with respect to the intrinsic platform yaw rotation the joint offsets can be neglected and each of the six link chains are in this paper modeled with one parameter only, namely the link length. The length of the lower arm link L_i, between joint positions u_i and p_i is named l_i.

IV. KINEMATIC EQUATIONS

A. Length equations

To decide expressions for the inverse and forward kinematics the starting point is the length equations for the lower arm links. Squaring these equations leads to (6). To save space the notation ${}^{F}p_{ij}$ has been shortened to p_{ij} and ${}^{F}u_{ij}$ to u_{ij}.

$$
e_i = (p_{ix} - u_{ix})^2 + (p_{iy} - u_{iy})^2 + (p_{iz} - u_{iz})^2 - l_i^2 = 0 \tag{6}
$$

Equation systems of this type are typical when deriving PKM kinematics. Normally the forward kinematics problem does not have a unique solution and a large effort has been made by the research community trying to find closed form solutions for different parallel manipulators.

In the general 6 DOF case 6 arbitrarily placed actuated joint positions would be connected through 6 passive links of given lengths to 6 arbitrarily placed positions on a moving platform. The solution to the forward kinematics problem means deciding the possible platform poses knowing the actuated joint positions. Many authors, for example [15] and [16], have shown that this problem has at the most 40 solutions, counting also non-realizable solutions in the complex domain. Algorithms to decide these solutions have been developed by for example [17]. Since it is difficult and

time consuming to find analytical solutions to the general forward kinematics problem for parallel robots numerical methods are often used.

If the parallelograms and universal joints are not assumed to be perfect, calculating the forward kinematics of the SCARA-Tau robot variants is an example of the general problem discussed above and therefore very difficult. For the triangular link SCARA-Tau no simple analytical solution to the forward kinematics has been found even if perfect parallelograms and joints are assumed while for the SCARA-Tau prototype the forward kinematics for the nominal design is straightforward.

Compared to serial type robots the solution to the inverse kinematics for PKMs is usually simple but the coupling of tool platform position and orientation makes also the solution to the inverse kinematics for the SCARA-Tau variants complicated. However, for the nominal design, when perfect parallelograms and joints are assumed, analytical solutions for both SCARA-Tau variants become more apparent.

B. Nominal model

For the triangular link SCARA-Tau the center points of the joint positions u_1, u_2 and u_3 are placed on a line. Nominally, the tool platform of this variant will have constant pitch and roll angles while its yaw angle will be dependent on the platform position projected in the xy-plane. For this to be true the links L_1 and L_2 have to be parallel and of equal length and the vertical distances u_1 - u_3 and u_2 - u_3 must be equal to the vertical distances p_1 - p_3 and p_2 - p_3. Also the links L_4 and L_5 must be parallel and of equal length. The platform orientation for the proposed triangular link SCARA-Tau is defined by Euler ZYZ rotation and can be represented by

$$\begin{aligned} \phi &= \frac{\pi}{2} + q_1 - \phi_t + \phi_r + \Delta\phi \\ \theta &= \frac{\pi}{2} + \Delta\theta \\ \psi &= \Delta\psi \end{aligned} \tag{7}$$

The angle ϕ_t represents a constant rotation. It is the angle between the front plane of the platform and the plane formed by the joint positions p_1, p_2 and p_3. The value can be decided from $\phi_t = arctan(-p_{6z}/p_{6y})$. The term ϕ_r is defined by the rotation of the links L_1, L_2 and L_3 around axis R in Fig. 3. If the conditions of perfect joints and parallelograms are true the three delta values are constant and for the nominal design these values are also zero.

In the nominal design of the SCARA-Tau prototype the links L_2 and L_3 form a perfect horizontal parallelogram, which means that its yaw angle is only dependent on the angle q_1. For the nominal design of the SCARA-Tau prototype the same representation of its platform orientation as (7) can be used if the angle ϕ_r is set to zero.

C. Inverse Kinematics

The nominal condition of perfect vertical parallelograms means that the first and second equation as well as the fourth and fifth equation in (6) are linearly dependent and it is enough to use only one of each to decide the solution. Introducing parameters c_{ij}, which have expressions too long to be included in this paper, equations 1, 3, 4 and 6 in (6) can be written as

$$\begin{aligned} &c_{11} + c_{12}sin(q_1) + c_{13}cos(q_1) = 0 \\ &c_{31}(q_1) + c_{32}(q_1)sin(\phi_r) + c_{33}(q_1)cos(\phi_r) = 0 \\ &c_{41}(q_1,\phi_r) + c_{42}(q_1,\phi_r)sin(q_2) + c_{43}(q_1,\phi_r)cos(q_2) = 0 \\ &c_{61}(q_1,\phi_r) + c_{62}(q_1,\phi_r)sin(q_3) + c_{63}(q_1,\phi_r)cos(q_3) = 0 \end{aligned} \tag{8}$$

These equations have the solution (9). After deciding the angle q_1 from the first equation in (8) the second equation is used to decide ϕ_r before calculating q_2 and q_3. To save space the dependency of the parameters c_{ij} on q_1 and ϕ_r shown in (8) is not written out explicitly in (9).

$$\begin{aligned} q_1 &= -2arctan\left(\frac{c_{12} \pm \sqrt{-c_{11}^2 + c_{12}^2 + c_{13}^2}}{c_{11} - c_{13}}\right) \\ \phi_r &= -2arctan\left(\frac{c_{32} \pm \sqrt{-c_{31}^2 + c_{32}^2 + c_{33}^2}}{c_{31} - c_{33}}\right) \\ q_2 &= -2arctan\left(\frac{c_{42} \pm \sqrt{-c_{41}^2 + c_{42}^2 + c_{43}^2}}{c_{41} - c_{43}}\right) \\ q_3 &= -2arctan\left(\frac{c_{62} \pm \sqrt{-c_{61}^2 + c_{62}^2 + c_{63}^2}}{c_{61} - c_{63}}\right) \end{aligned} \tag{9}$$

The inverse kinematics gives 16 solutions. The valid solution is decided by first choosing the smallest value of q_1 and then deciding the solution of ϕ_r with the smallest absolute value and finally selecting the largest values of q_2 and q_3 found using the chosen solutions of q_1 and ϕ_r.

For the SCARA-Tau prototype the links L_1, L_2 and L_3 nominally form a perfect double parallelogram. This means that the first three equations in (6) are all linearly dependent and instead of using the third equation to decide ϕ_r, this value is set to zero when calculating the parameter values $c_{ij}(q_2,\phi_r)$ needed for the solutions of q_2 and q_3 in (9).

D. Forward Kinematics

No simple analytical solution to the forward kinematics of the proposed triangular link SCARA-Tau has been found.

For the SCARA-Tau prototype the nominal forward kinematics is solved by introducing parameters d_{ij}, which are functions of the robot parameters and the joint angles q_1, q_2 and q_3 but too long to be included here. By setting the value of ϕ_r to zero the equations 1, 4 and 6 from (6) can be written

$$\begin{aligned} &x^2 + y^2 + z^2 + d_{11}x + d_{12}y + d_{13}z + d_{10} = 0 \\ &x^2 + y^2 + z^2 + d_{41}x + d_{42}y + d_{43}z + d_{40} = 0 \\ &x^2 + y^2 + z^2 + d_{61}x + d_{62}y + d_{63}z + d_{60} = 0 \end{aligned} \tag{10}$$

The quadratic terms can be eliminated by subtracting the third equation from the two first equations, thereby creating 2 linear equations from which x and y can be decided as expressions of z. Inserting these expressions in the first equation in (10) finally gives a value of z. By introducing more parameters according to

$$
\begin{aligned}
e_1 &= (d_{13}-d_{63})(d_{42}-d_{62})-(d_{12}-d_{62})(d_{43}-d_{63})\\
e_2 &= (d_{10}-d_{60})(d_{42}-d_{62})-(d_{12}-d_{62})(d_{40}-d_{60})\\
e_3 &= (d_{11}-d_{61})(d_{43}-d_{63})-(d_{13}-d_{63})(d_{41}-d_{61})\\
e_4 &= (d_{11}-d_{61})(d_{40}-d_{60})-(d_{10}-d_{60})(d_{41}-d_{61})\\
e_5 &= (d_{12}-d_{62})(d_{41}-d_{61})-(d_{11}-d_{61})(d_{42}-d_{62})\\
f_1 &= 2(e_1^2+e_3^2+e_5^2)\\
f_2 &= e_2^2+e_4^2+d_{11}e_2e_5+d_{12}e_4e_5+d_{10}e_5^2\\
f_3 &= -(2e_1e_2+2e_3e_4+d_{11}e_1e_5+d_{12}e_3e_5+d_{13}e_5^2)\\
g_1 &= \sqrt{f_3^2-2f_1f_2}
\end{aligned}
\tag{11}
$$

the solution can be written

$$
z=\frac{f_3\pm g_1}{f_1},\quad y=\frac{e_3z+e_4}{e_5},\quad x=\frac{e_1z+e_2}{e_5} \tag{12}
$$

The angles of the upper arms (q_i) decide which of the two solutions in (12) that is valid.

E. Constraints on the solutions

In addition to choosing the correct solutions from equations (9) and (12), other constraints on a valid solution are needed because of joint limitations and to avoid collisions between the lower arms and the base. This is done by calculating the horizontal elbow angles α_{hi} and the vertical elbow angles α_{vi}, as shown in (13), and limiting these angles.

$$
\begin{aligned}
v_i &= -{}^F u_i,\quad w_i = {}^F p_i - {}^F u_i\\
\alpha_{vi} &= \arctan\left(\frac{w_i(3)}{\sqrt{w_i(1)^2+w_i(2)^2}}\right)\\
\alpha_{hi} &= \arccos\left(\frac{v_i(1)w_i(1)+v_i(2)w_i(2)}{\sqrt{(v_i(1)^2+v_i(2)^2)(w_i(1)^2+w_i(2)^2)}}\right)
\end{aligned}
\tag{13}
$$

V. Comparison of the SCARA-Tau variants

A. Platform orientation and workspace

Optimal platform yaw angle is dependent on where the tool, or wrist, is mounted on the platform. An optimal yaw angle means a platform orientation that in all positions in the workspace form a 90 degree angle with a radial line passing through the center of the cylindrical column and the point on the platform where the tool or wrist is mounted. Such a radial line has been plotted in Fig. 2(a) and Fig. 2(b). If the tool is placed in $[x_T, y_T, z_T]$ the corresponding optimal yaw angle, ϕ_o, is given by

$$
\begin{aligned}
\phi_o &= arccos\left(\frac{x_T}{\sqrt{x_T^2+y_T^2}}\right),\quad y_T \geq 0\\
\phi_o &= 2\pi - arccos\left(\frac{x_T}{\sqrt{x_T^2+y_T^2}}\right),\quad y_T < 0
\end{aligned}
\tag{14}
$$

It is easy to modify the platform design to reduce or increase the platform yaw angle by a constant value so that the mean deviation between the actual platform yaw angle and optimal yaw angle is zero over the workspace. What can not be controlled is how much the platform orientation deviates from this mean value. The main benefit of the triangular link SCARA-Tau variant is to reduce this variation which will be shown in this section.

Even though the optimal yaw angle is dependent on where a tool is placed on the platform it still only gives a constant offset to the results. Since it is easy to reduce or increase the platform yaw angle with a constant value it is enough to use $[x_T, y_T, z_T] = [x, y, z]$ while studying the platform orientation for the prototype and the proposed modification.

In Fig. 4 the derived inverse kinematics have been used to plot side views of the reachable workspace for the two SCARA-Tau variants. Since all three actuated arms rotate around a common axis the same workspace as plotted can be reached in any radial direction which creates a large doughnut-shaped workspace.

Fig. 4(a) and Fig. 4(c) show the workspace for the SCARA-Tau prototype while in Fig. 4(b) and Fig. 4(d) the workspace of the proposed triangular link SCARA-Tau robot is displayed. In Fig. 4(a) and Fig. 4(b) the used lower arm link lengths are the same as for the SCARA-Tau prototype while in Fig. 4(c) and Fig. 4(d) 30% longer links are used.

All reachable positions have been plotted and in each position the platform yaw angle, ϕ, has been calculated according to (7). The difference between the actual yaw angle and the optimal yaw angle, according to (14), has been calculated in each position. A mean value of this deviation ϕ_m, calculated in N points over the whole robot workspace, has been calculated for each plot according to

$$
\phi_m = \frac{1}{N}\sum_{i=1}^{N}(\phi_i - \phi_{oi}) \tag{15}
$$

Each position has then been colored according to the absolute value of the difference between actual yaw angle and optimal yaw angle, after the mean value, ϕ_m, has been subtracted from the actual yaw angle. The reason for subtracting the mean value is that it only represents a constant offset that is dependent on where the tool is placed on the platform and could be easily removed by small changes in the platform design. The lightest color is used for deviations of less than 10 degrees, the second lightest color for deviations between 10 and 30 degrees, while the black color signifies a deviation larger than 30 degrees.

Fig. 4(a) shows the results for the SCARA-Tau prototype. As can be seen, the smallest deviation from optimal yaw angle is found in the central part of the workspace, while the deviation increases for positions further away from the central region, and becomes larger than 30 degrees at the inner and outer limits of the prototype workspace. The plot in Fig. 4(c) is also for the SCARA-Tau prototype and shows the results when the lower arm link lengths have been increased by 30% compared to the lengths used for the prototype. Except for the change in reachable workspace the plot is similar to Fig. 4(a) and no major changes in platform orientation compared to that case are obvious.

Fig. 4(b) shows the results for the proposed triangular link variant when equal arm lengths as the prototype are used. As can be seen, the deviation from optimal platform orientation has been reduced significantly compared to the prototype. The size of the region with a deviation of less than 10 degrees has increased and the region with a deviation larger than 30 degrees has almost disappeared. The plot in Fig. 4(d) is also for the proposed triangular link variant. Here the lengths of the lower arm links have been increased by 30%. As can be seen, using these longer links makes the advantage of the triangular link SCARA-Tau variant even larger. The majority of the workspace now has a deviation of less than 10 degrees from optimal yaw angle.

The four thicker horizontal lines on the cylindrical base mark the six joint positions u_i on the upper arms. The order of the joints, starting from the bottom, is 3, 2&4, 1&5, 6 for the prototype and 2&4, 3, 1&5, 6 for the triangular variant. Note that the fixed coordinate system is placed at the same height as joint position u_3 which for the triangular variant is 0.16 meters higher compared to the prototype. The flat top and bottom of the workspace depend on the limitations of the vertical working range of the universal joints. The joints are normally mounted angled to maximize the lower part of the workspace.

One important observation that can be made from the plots in Fig. 4 is that the work area below the lowest of the joint positions u_i is free from upper arms. This means that this section of the work area is ideal to use in for example pick-and-place applications in the negative z-direction. For these applications it is important to maximize the workspace below the joint positions on the upper arms and, as can be seen in Fig. 4(c) and Fig. 4(d), one way to achieve this goal is to increase the lengths of the lower arm links. An additional increase of the lower part of the workspace can be obtained by moving the joint positions u_1, u_2 and u_3 so that the line R in Fig. 3 is tilted downwards. A corresponding change is then also needed for the joint positions u_4 and u_5.

In Fig. 5 the difference in platform orientation between the two variants is shown in more detail. The same four variants as in Fig. 4 are compared. The deviation from optimal yaw angle has been calculated as in Fig. 4 but is here plotted as a function of the radial distance from the center of the cylindrical base column at the constant height 0.9 meter from the bottom of the base column.

When increasing the lower arm link lengths the reachable

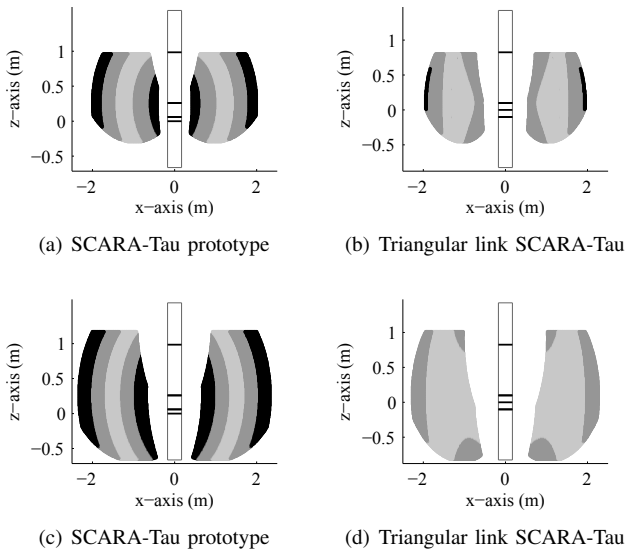

(a) SCARA-Tau prototype (b) Triangular link SCARA-Tau

(c) SCARA-Tau prototype (d) Triangular link SCARA-Tau

Fig. 4. Figures (a) and (c) show the reachable workspace for the SCARA-Tau prototype seen from the side while the figures (b) and (d) show the same views for the proposed triangular link SCARA-Tau. In figures (a) and (b) the used lower arm link lengths are the same as used for the SCARA-Tau prototype while in figures (c) and (d) 30% longer links are used. The plots are colored according to the deviation from optimal yaw angle where darker color means larger deviation. The four thicker horizontal lines on the cylindrical base mark the height of the six joint positions u_i on the upper arms.

workspace is moved further away from the central column. This is true for both the SCARA-Tau prototype and the proposed triangular variant. In the plot the reachable workspace of the triangular variant is smaller than for the prototype. This is an effect of placing the center of the tool coordinate system in joint position p_1. If it was instead placed in joint position p_5 the workspace of the triangular variant would be the largest while the workspace of the two variants would be similar if the center of the tool coordinate system was placed in the middle of the platform, between the joint positions p_1 and p_5.

The value displayed in the plots is $D_\phi = \phi - \phi_m - \phi_o$. This value should be as close to zero as possible. A measure $V_\phi = max(D_\phi) - min(D_\phi)$ is introduced to describe the maximum variation of D_ϕ at constant height. Since the robot has rotational symmetry it is enough to decide V_ϕ along a radial line. Along such a line the optimal yaw angle, ϕ_o, is always constant which means that by using (7) the expression for V_ϕ can be simplified to

$$V_\phi = max(q_1 + \phi_r(q_1)) - min(q_1 + \phi_r(q_1)) \qquad (16)$$

Note that the formula above is valid also for the SCARA-Tau prototype using $\phi_r = 0$. As can be seen if comparing the solid line and the dashed line in Fig. 5, using longer lower arm links for the prototype gives a larger variation of platform orientation. The reason for this is that the use of longer lower arm links makes the upper arms work behind the central column when the platform is close to the column. This means a smaller minimum value of the

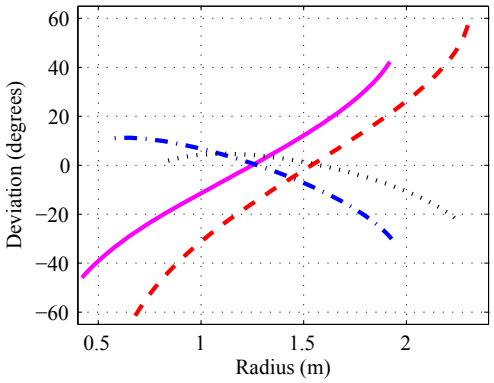

Fig. 5. Deviation from optimal yaw angle as a function of the radial distance from the center of the base column. The solid line shows the result for the SCARA-Tau prototype and the dashed line the result for the same prototype using 30% longer lower arm links. The dashed-dotted line shows the result for the proposed triangular variant using the same arm lengths as the prototype and the dotted line the result for the triangular variant using 30% longer lower arm links.

angle q_1, which according to (16) means a larger span of the platform orientation.

Also for the proposed triangular link variant using longer lower arm links means that the upper arms work behind the central column when the platform is close to the column. However, in this case the smaller values of q_1 are compensated for by the angle ϕ_r so that the resulting total platform deviation is less compared to the case when using shorter lower arm links. See the dotted-dashed plot and the dotted plot respectively.

VI. Conclusion and Future Work

The large workspace and similarities to a robot with serial kinematics makes the SCARA-Tau structure a very promising PKM. In this paper the inverse kinematics of a proposed triangular link modification of the SCARA-Tau has been derived and it has been demonstrated that the proposed modification significantly reduces the dependence between platform position and orientation. Since the platform reorientation would limit the useful workspace for certain applications, the proposed modification will open up possibilities for even more applications where the SCARA-Tau robot could be useful.

The complete kinematics for the SCARA-Tau variants derived in this paper will be used to identify kinematic error parameters so they can be compensated for in software. For compensation of the platform orientation errors either a wrist or a possibility to manipulate the lengths of three of the lower arm links is needed. In the latter case telescopic actuators could be utilized and these actuators could also be used to control the platform orientation in applications where a large range of controllable platform orientation is not essential. The platform yaw angle could be controlled by replacing the lower arm link L_3 with a telescopic link. Since the proposed triangular link variant has less inherent variation of the yaw angle compared to the original SCARA-Tau concept it is well suited to this modification. The range of achievable controlled yaw angle for this variant would be similar in all positions. Planned future work includes evaluating the possibilities of increasing the DOFs of the SCARA-Tau robot by using telescopic lower arm links.

For the original SCARA-Tau concept the horizontal parallelogram is approaching its working range boundaries in the regions close to the inner and outer workspace limits of the robot while this is not an issue for the triangular link variant. This advantage of the triangular link SCARA-Tau is even more pronounced when longer lower arm links are used. Therefore, it would be of great interest to compare the elastostatic properties of the two variants.

If further studies confirm the advantages of the triangular link variant, it is a relatively minor change to rebuild the present SCARA-Tau prototype to incorporate this change.

References

[1] J. P. Merlet, "Merlet homepage." [Online]. Available: http://www-sop.inria.fr/members/Jean-Pierre.Merlet/Archi/archi_robot.html

[2] F. Rehsteiner, R. Neugebauer, S. Spiewak, and F. Wieland, "Putting Parallel Kinematics Machines (PKM) to Productive Work," *CIRP Annals - Manufacturing Technology*, vol. 48, no. 1, pp. 345–350, 1999.

[3] T. Brogårdh, "PKM Research - Important Issues, as seen from a Product Development Perspective at ABB Robotics," in *Workshop on Fundamental Issues and Future Research Directions for Parallel Mechanisms and Manipulators*, Quebec City, Quebec, Canada, 2002.

[4] R. Clavel, "Dispositif pour le déplacement et le positionnement d'un élément dans l'espace," Patent CH 672089, 1985.

[5] T. Brogårdh, "Design of high performance parallel arm robots for industrial applications," in *Proceedings of a Symposium Commemorating the Legacy, Works, and Life of Sir Robert Ball Upon the 100th Anniversary of A Treatise on the Theory of Screws*, University of Cambridge, Trinity College, 2000, pp. 9–11.

[6] S. Kock, R. Oesterlein, and T. Brogårdh, "Industrial robot," Patent WO 03/066289, 2003.

[7] H. Cui, Z. Zhu, Z. Gan, and T. Brogårdh, "Kinematic analysis and error modeling of TAU parallel robot," *Robotics and Computer Integrated Manufacturing*, vol. 21, no. 6, pp. 497–505, 2005.

[8] T. Brogårdh, S. Hanssen, and G. Hovland, "Application-Oriented Development of Parallel Kinematic Manipulators with Large Workspace," in *2nd International Colloquium of the Collaborative Research Center 562: Robotic Systems for Handling and Assembly*, Braunschweig, Germany, 2005, pp. 153–170.

[9] T. Brogårdh, I. Lundberg, and D. Wäppling, "A parallel kinematic manipulator and a method for operating the same, including pair wise actuators," Patent WO 2004/056538, 2004.

[10] T. Brogårdh, "Parallel kinematic robot and method for controlling this robot," Patent US 2007/0255453, 2007.

[11] G. Hovland, M. Choux, M. Murray, I. Tyapin, and T. Brogårdh, "The Gantry-Tau - Summary of Latest Development at ABB, University of Agder and University of Queensland," in *the 3rd Intl. Colloquium: Robotic Systems for Handling and Assembly, the Collaborative Research Centre SFB 562*, Braunschweig, Germany, 2008.

[12] I. Dressler, M. Haage, K. Nilsson, R. Johansson, A. Robertsson, and T. Brogårdh, "Configuration Support and Kinematics for a Reconfigurable Gantry-Tau Manipulator," in *IEEE International Conference on Robotics and Automation (ICRA'07)*, Roma, Italy, 2007.

[13] "Schaeffler group homepage." [Online]. Available: http://www.schaeffler.us/content.schaeffler.us/us/ina_fag_products/

[14] "SMErobot homepage." [Online]. Available: http//www.smerobot.org

[15] J. C. Faugére and D. Lazard, "Combinatorial classes of parallel manipulators," *Mechanism and Machine Theory*, vol. 30, no. 6, pp. 765–776, 1995.

[16] C. W. Wampler, "Forward displacement analysis of general six-in-parallel SPS (Stewart) platform manipulators using soma coordinates," *Mechanism and Machine Theory*, vol. 31, no. 3, pp. 331–337, 1996.

[17] M. L. Husty, "An Algorithm for Solving the Direct Kinematic Of Stewart-Gough-Type Platforms," *Mechanism and Machine Theory*, vol. 31, no. 4, pp. 365–379, 1996.